551.511 : 551.576.11

Models of cloud-topped mixed layers under a strong inversion

By D. K. LILLY

National Center for Atmospheric Research, Boulder, Colorado

(Manuscript received 3 July 1967; in revised form 29 January 1968)

SUMMARY

Theoretical models are constructed with the aim of relating, explaining and predicting features of a radiatively active turbulent cloud layer over the sea and under a strong subsidence inversion. Both dry aerosol clouds (no phase change) and wet clouds (with a phase change and latent heat exchanges) are considered. For the wet cloud case an important element of the theory is the requirement that the wet-bulb potential temperature must increase upwards in the inversion. For both cases entrainment of the upper warm air is hypothesized to lie between upper and lower limits determined from the turbulent energy budget. The dry cloud case is solved for both steady state and transient results, with only the transient behaviour depending on the entrainment hypothesis. Only steady state solutions are presented for the more complex wet cloud case and these differ somewhat for the maximum and minimum entrainment limits. Observational data from Oakland, California are used for comparison with those steady state solutions, with results indicating the essential validity of the approach. Detailed comparisons, especially for determination of the most correct entrainment rate, are hampered both by inadequate measurement of the inversion properties and by uncertainties in the net radiation flux leaving the cloud top. Computations of the latter suggest that several presently used radiation models are still in serious disagreement, at least for application to downward flux under an inversion. It is suggested that the present theory provides a partial explanation of the origin of the trade wind inversion.

1. PHYSICAL FRAMEWORK AND MOTIVATION

A shallow turbulent moist stratum is characteristic of Equatorward flow just above the middle-latitude and tropical oceans, especially at the eastern ends of sub-tropical high pressure areas of the eastern North and South Pacific and South Atlantic oceans. This moist stratum, or marine layer, is typified by a solid or broken cloud cover, topped by a strong temperature inversion with warm dry air aloft. The extreme sharpness of the inversion, observed strikingly in kite soundings from the Meteor expedition (von Ficker 1936, examples presented by Riehl 1954), is normally partly concealed by the instrumental lag in balloon-borne radiosondes. It has often been revealed further, however, by instrumented airplane flights (James 1959; Edinger 1963, 1966) and slow-ascent radiosondes (Williams and De Mandel 1966).

Qualitative explanations for this régime, offered for many years (Petterssen 1938; Riehl 1954, Chapter 2; Neiburger 1944), were based on the following arguments. In conditions of strong or moderate subsidence the potential temperature of the lower troposphere may be substantially higher than that of the ocean surface. Since the ocean has effectively an almost infinite heat capacity, a temperature inversion or stable layer must form somewhere. The turbulence generated by surface shear could be expected to mix the lower layer and maintain a sharp, somewhat elevated inversion, while radiation from the top of a cloud would exert an additional cooling effect in the mixed layer.

In recent years the effect of stratification on the surface boundary layer has been clarified somewhat by observation and theoretical analysis. In particular, the length scale introduced by Monin and Obukhov is shown to act as an upper bound on the influence of surface shear-generated turbulence. Since this scale is not often greater than a few tens of meters, it seems that we must deny the importance of surface shear in the maintenance of a mixed layer 500 to 1,000 meters or more in thickness.

In the present theory we therefore disregard the effects of the surface shear-generated turbulence but consider radiation off the cloud tops as an essential element. In this respect we follow Petterssen, who particularly emphasized the radiative heat loss. This theory may not be valid for the occasionally observed cases of extremely shallow (< 100 m)

marine layers without condensation, but is intended to hold for the fog-, stratus- or stratocumulus-containing layer typically observed near the coast of California in the summer, and near northern Chile, southern Peru and South West Africa most of the year.

A further essential foundation of the present theory is the stability of the cloud top against penetration by the very dry upper air mass. If a parcel of the upper air is introduced into the cloud layer and mixed by turbulence, evaporation of cloud droplets into the dry parcel will reduce its temperature. If the mixed parcel reaches saturation at a colder temperature than that of the cloud top it will be negatively buoyant and can then penetrate freely into the cloud mass. In such a case the evaporation and penetration process will occur spontaneously and increase unstably until the cloud is evaporated. The condition for no change in temperature upon evaporative mixing is that the wet-bulb potential temperatures of the wet and dry layers be equal. We assume, therefore, that for stability of a cloud layer the inversion at its top must be sufficiently strong that the wet-bulb potential temperature remains constant or increases upward at the cloud top. For a difference of 5-10 g/kg in mixing ratio between mixed layer and upper dry layer this requires $\sim$13-26°C increase in potential temperature across the inversion. Such inversion strengths are commonly observed in west coast soundings and it appears, on the basis of somewhat inadequate data, that the theoretical requirement is usually satisfied.

We further assume that the large-scale vertical motion and the upper air (above the inversion) temperature and humidity structure are known, as well as the near-surface wind, surface temperature, and (saturated) surface humidity. Certain simplified formulations are used for calculating surface heat and moisture fluxes and radiative heat-flux. Precipitation is neglected, which probably restricts the application to rather thin and not too cold cloud layers.

The interaction of large-scale atmospheric properties and thermal convection is a principal unsolved problem in the development of forecast and/or general circulation models. The phenomenon considered here represents one form, in some respects a relatively simple one, of this interaction. There is a considerable lack of highly definitive observational data on layered convection, in fact on most kinds of non-violent cloud convection. A principal motivation for this work was to sharpen the questions to be asked and to help avoid purely exploratory observations, which may already exist in sufficient abundance.

2. A SIMPLIFIED DRY 'CLOUD' LAYER

As a simplified illustration of the mechanism which will be explored more realistically in the next section, we consider a shallow radiation-absorbing cloud of dust, smoke, or other inert matter occupying the lower part of a horizontally homogeneous air mass subject to a specified large-scale vertical motion field $w(z) \leqslant 0$. Radiative cooling is occurring in the air above the cloud at a rate which will maintain a stable potential temperature profile $\theta_U(z)$, i.e., $\partial\theta_U/\partial z > 0$. The upper layer above the cloud is assumed to be non-turbulent. The lower boundary, the Earth's surface, is maintained at a potential temperature θ_S. Turbulent heat-flux from the surface is assumed proportional to the near-surface wind and to the surface-air temperature difference through a heat transfer coefficient C_T, that is

$$(\overline{w'\theta'})_0 = C_T V_0 (\theta_S - \theta_0), \quad . \quad . \quad . \quad . \quad (1)$$

where θ_0 is the potential temperature of the air at a small height above the surface. If this heat transfer is positive it is assumed that the entire cloud layer, from the surface to $z = H$, is well mixed at a very high Rayleigh number, and is therefore nearly isentropic with potential temperature θ_0 except very close to the boundaries. At the top of the cloud layer a net outward radiative heat flux F_{UH} tends to cool the top, and therefore the entire cloud layer.

We now proceed to derive expressions for the time rates of change of θ_0 and H, as functions of their initial conditions and the values of w, F_{UH} and θ_U, considered as

external parameters. It will become clear that in order to do this it is necessary to make an assumption about the ability of convection to penetrate a stable layer.

Under the assumption that H is much smaller than the scale height of the atmosphere, Ogura and Phillips (1962) have shown that it is possible to use the Boussinesq approximation, but with potential temperature replacing temperature as the thermal variable. The thermal equation for the cloud layer is then a simple one; i.e.

$$\frac{\partial \theta_0}{\partial t} = -\frac{\partial}{\partial z}(\overline{w'\theta'}). \quad . \quad . \quad . \quad . \quad . \quad (2)$$

Since θ_0 is constant with height, this implies that the turbulent heat transport is a linear function of height, that is, that

$$\overline{w'\theta'} = \left(1 - \frac{z}{H}\right)(\overline{w'\theta'})_0 + \frac{z}{H}(\overline{w'\theta'})_H \quad . \quad . \quad . \quad (3)$$

so that Eq. (2) may also be written

$$\frac{\partial \theta_0}{\partial t} = [(\overline{w'\theta'})_0 - (\overline{w'\theta'})_H]/H. \quad . \quad . \quad . \quad . \quad (4)$$

The subscript H refers to properties of the cloud layer just under its top. The subscript UH will refer to properties just above the top. Relative to the moving surface, $z = H$, the fluid has a motion $w_H - \partial H/\partial t$, so that if a stable temperature discontinuity exists it must be maintained by an infinite heating or cooling rate, associated with a discontinuity in the radiative and/or turbulent heat-fluxes. We express this by the following heat balance equation at the layer top :

$$\left(\frac{\partial H}{\partial t} - w_H\right)(\theta_{UH} - \theta_0) + (\overline{w'\theta'})_H = F_{UH}. \quad . \quad . \quad (5)$$

Eq. (5) may be formally derived in the following manner. Assume that in a layer of constant thickness ΔH enveloping the cloud top the mean flow advection and the turbulent and net radiative heat-fluxes are all of comparable and finite magnitude, so that the potential temperature equation is

$$\frac{\partial \theta}{\partial t} = -w_H \frac{\partial \theta}{\partial z} - \frac{\partial}{\partial z}(\overline{w'\theta'}) - \frac{\partial F}{\partial z}.$$

Integrate this equation through its depth of validity, that is from $z = H - \Delta H/2$ to $z = H + \Delta H/2$, to obtain

$$\int_{H_-}^{H_+} \frac{\partial \theta}{\partial t}\, dz = -w_H(\theta_{UH} - \theta_0) + (\overline{w'\theta'})_H - F_{UH}$$

where the limits of integration have been abbreviated in the left-hand term. Expand this term to the form

$$\int_{H_-}^{H_+} \frac{\partial \theta}{\partial t}\, dz = \frac{\partial}{\partial t}\int_{H_-}^{H_+} \theta\, dz - \frac{\partial H}{\partial t}(\theta_{UH} - \theta_0).$$

Upon going to the limit $\Delta H = 0$ the first term on the right vanishes and the desired relation is obtained.

Eqs. (1), (4) and (5) contain four unknowns, θ_0, H, $(\overline{w'\theta'})_0$ and $(\overline{w'\theta'})_H$. Thus there is no unique solution. A single steady-state solution exists, in which $(\overline{w'\theta'})_H = (\overline{w'\theta'})_0$ and H does not appear explicitly. It should be noted, however, that θ_U and w are both functions of z, so that H must be arbitrarily specified. It is clear that the equation needed

to close the system must be one which predicts the rate of turbulent entrainment at the cloud top, presumably from consideration of the turbulent energy balance. When a turbulent body of fluid is in contact with a non-turbulent region, the boundary between them remains sharp but the non-turbulent fluid is entrained into and made part of the turbulent fluid. In the present case the turbulent energy of the mixed layer is produced by buoyant forces associated with upward heat-flux. We now proceed to formulate quantitatively the relationship between entrainment and the turbulent energy balance, basically following the work of Ball (1960).

The turbulent energy equation, integrated over the mixed layer depth may be written

$$\int_0^H \left(\frac{\partial E}{\partial t} + w\frac{\partial E}{\partial z}\right) dz = g\int_0^H \frac{\overline{w'\theta'}}{\bar{\theta}}\, dz - (\overline{w'E'})_H - \int_0^H \epsilon\, dz \quad . \quad (6)$$

where $E = \overline{\mathbf{v}'^2}/2$, the turbulent kinetic energy, ϵ is the rate of molecular dissipation, and $\overline{w'E'}$ is a shorthand notation for the pressure-velocity and triple velocity product terms. The generation and dissipation of shear-driven turbulence in the lowest levels has been ignored for reasons stated in the previous section. We next offer an argument that the terms on the left-hand side of Eq. (6) are negligibly small compared to those on the right-hand side.

Measurement of various turbulent flows with a well-defined length scale L support the dimensional relation

$$\bar{E}^{3/2}/\bar{\epsilon} = \text{constant} \times L, \quad . \quad . \quad . \quad . \quad (7)$$

where the bars denote average values and the constant is of order unity. Assuming that the first and third terms on the right-hand side of Eq. (6) are of the same order, and specifying $H = L$, we obtain a time scale τ_E for variations of kinetic energy of order $\bar{E}$.

$$\tau_E = \frac{\bar{E}}{\bar{\epsilon}} \approx \left(\frac{H^2}{\bar{\epsilon}}\right)^{1/3} \sim \left(\frac{H^2}{g\,\overline{w'\theta'}/\bar{\theta}}\right)^{1/3} . \quad . \quad . \quad . \quad (8)$$

For realistic values of heat-flux and shallow layer depths τ_E is of order 10^3 sec, the time scale of a single convective cell. Thus if the heat-flux remains essentially constant, a quasi-steady state will be attained in the kinetic energy equation in well under an hour We show later in this section that the heat-fluxes and layer depth typically change much more slowly, with a time constant of order $H/C_T V_0 \sim 1$ day, so that use of the steady-state energy equation is justified *a posteriori*. Similarly we can easily reject the vertical advection term as small compared to dissipation. Eq. (6) then becomes

$$-g\int_0^H \frac{\overline{w'\theta'}}{\bar{\theta}}\, dz + (\overline{w'E'})_H + \int_0^H \epsilon\, dz = 0. \quad . \quad . \quad . \quad (9)$$

Ball hypothesized that the dissipation and transport terms of (9) are negligibly small compared to opposing positive and negative contributions to the energy conversion terms, so that

$$\int_0^H \overline{w'\theta'}\, dz = 0 \quad \text{but} \quad \overline{w'\theta'} \neq 0 \quad \text{somewhere.} \quad . \quad . \quad (10)$$

Although laboratory measurements of individual thermal elements (Richards 1963) suggest that substantial amounts of turbulent energy are dissipated almost immediately, Ball's hypothesis clearly corresponds to an upper possible limit on the entrainment of warm air from above. For a linearly varying heat-flux, as in (3), Ball's hypothesis leads to the result

$$(\overline{w'\theta'})_H = -(\overline{w'\theta'})_0. \quad . \quad . \quad . \quad . \quad . \quad (11)$$

That is, the heat transported down from above the inversion equals that carried up from

below. Upon combining Eqs. (11) and (1) with Eqs. (4) and (5) we obtain a closed set of equations for the maximum entrainment case :

$$\frac{\partial \theta_0}{\partial t} = 2\, C_T\, V_0\, (\theta_S - \theta_0)/H \quad . \quad . \quad . \quad . \quad (12)$$

$$\frac{\partial H}{\partial t} - w_H = \frac{F_{UH} + C_T\, V_0\, (\theta_S - \theta_0)}{\theta_{UH} - \theta_0} \quad . \quad . \quad . \quad (13)$$

The minimum possible entrainment is of course zero; that is, $\partial H/\partial t = w_H$. A restriction which we believe represents a more probable minimum on entrainment than zero, however, is that

$$(\overline{w'\theta'})_{\text{minimum}} = 0 \quad \text{but} \quad \int_0^H \overline{w'\theta'}\, dz > 0. \quad . \quad . \quad (14)$$

The effect of this restriction is to require that all energy dissipation occurs within the region of positive conversion from potential energy, no energy being transported to do work outside the boundaries of the positive conversion region. Recent laboratory studies of penetrative convection (Deardorff, Willis and Lilly 1968) showed results much closer to this condition than to that of Ball's hypothesis.

We will refer to Eqs. (11) and (14) as the maximum and minimum entrainment hypotheses. Since both of these hypotheses are based on use of the steady-state energy equation, Eq. (9), they must both be subject to the constraint that the turbulent fluid does not contain any source of mean internal buoyant instability and, in particular, that the temperature discontinuity at its top is a stable one, that is that

$$\theta_{UH} \geqslant \theta_0. \quad . \quad . \quad . \quad . \quad . \quad . \quad (15)$$

If this condition were violated, for example by an upper layer of substantial thickness having a temperature substantially lower than that of the mixed layer, this entire upper layer would sink through the mixed layer in the form of convective cells or bubbles with a time scale comparable to that of Eq. (8).

Applied to the above system (Eqs. (1), (4) and (5)), the minimum entrainment hypothesis leads to the minimum entrainment model equations,

$$\frac{\partial \theta_0}{\partial t} = C_T\, V_0\, (\theta_S - \theta_0)/H \quad . \quad . \quad . \quad . \quad (16)$$

$$\frac{\partial H}{\partial t} - w_H = F_{UH}/(\theta_{UH} - \theta_0). \quad . \quad . \quad . \quad . \quad (17)$$

We have chosen the zero value of $(\overline{w'\theta'})$ to be at the upper boundary $z = H$. The other possible case, $(\overline{w'\theta'})_0 = 0$, requires from Eq. (1) that $\theta_0 = \theta_S$, therefore from Eq. (4) that heat-flux vanishes everywhere, violating the second part of Eq. (14). In Table 1 we present a summary of the above derivations, together with those to be presented in the next section for wet clouds.

It should be noted that in any continuous solution of either the maximum or minimum entrainment model Eq. (15) always remains satisfied as an inequality. If the denominator of either Eqs. (13) or (17) becomes small, the entrainment rate increases, so that with a stable lapse rate above $z = H$ the inversion strength must then increase.

To illustrate the transient and steady-state behaviour of the two models we have performed numerical integrations of both for a given set of initial and environmental data. A constant divergence rate, a given upper level stability, a radiative cooling rate and other parameters are assumed typical of the California coastal conditions to be illustrated in

more detail in a later Section. Numerical values are

$$\left.\begin{aligned} \theta_{UH} &= 282°\text{K} + 5\ \text{deg/km} \times H, \qquad \theta_S = 285°\text{K} \\ w_H &= -0{\cdot}55 \cdot 10^{-5}\ \text{sec}^{-1} \times H, \qquad F_{UH} = 0{\cdot}06\ \text{deg m sec}^{-1} \\ C_T V_0 &= 0{\cdot}015\ \text{m sec}^{-1} \end{aligned}\right\}. \quad . \quad (18)$$

The initial conditions are $H = 0$, $\theta_0 = \theta_{U0}$, corresponding to an initially stable atmosphere moving out over a warmer surface. Fig. 1 shows the time-dependent behaviour of the solutions. In these the diagonal represents the initial stable lapse rate, while the verticals are the subsequent soundings through the mixed layer. The general development of the solution is similar for the two models, but in the maximum entrainment case the depth of the mixed layer grows substantially faster than it does in the minimum entrainment case. In both cases an inversion begins to form immediately and grows roughly in proportion to the growth of the mixed layer.

The steady-state solution for mixed layer depth H is obtained from solution of the quadratic resulting from substitution of Eq. (18) into the steady-state versions of Eqs. (16) and (17). The result, shown as the infinite limit on Fig. 1, is $H = 1{,}808$ m, and the inversion strength is $\theta_{UH} - \theta_0 = 6{\cdot}04°\text{C}$. It is interesting and curious that in the dry case this steady-state solution, with $\overline{w'\theta'} = 0$ everywhere, is the same for both models, but that in each case it violates the corresponding entrainment hypothesis. In actuality both radiation and entrainment operate over a finite depth rather than on a two-dimensional surface, so that the models become seriously oversimplified at the steady-state limit. This degeneracy of the steady-state solution does not occur in the moist cloud model. In any case, with arbitrary initial conditions and steady upper layer temperatures and subsidence rates, the steady-state solutions are actually asymptotic states which are approached exponentially.

It is tempting to seek a real physical situation corresponding to the above solutions, but none has occurred to the author. The obvious possibility of smoke-polluted air at night would not usually have a large enough surface heat-flux to generate convective overturning in a mixed layer unless it drifted over a water surface.

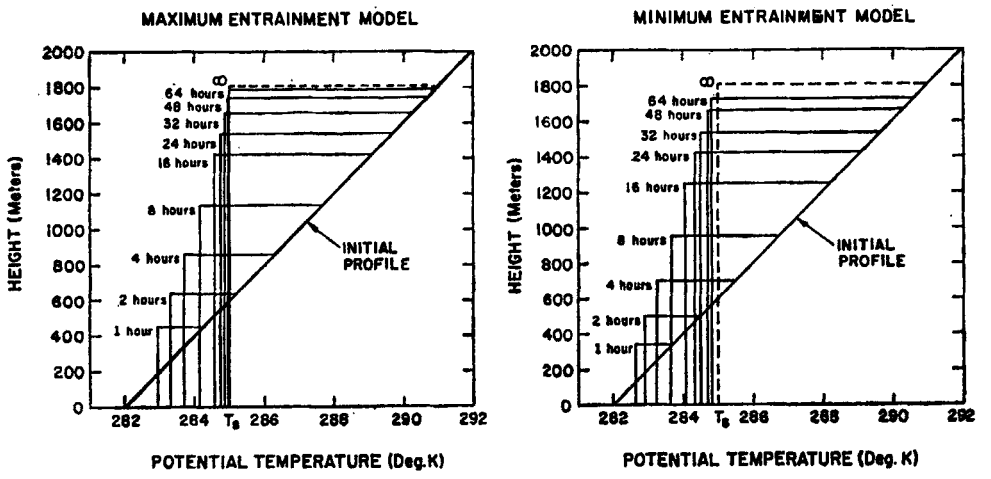

Figure 1. Time-dependent solutions of the dry cloud model for maximum and minimum entrainment hypotheses. The diagonal line is the initial stable sounding, while the successive step functions represent development and ascent of the mixed layer and inversion top. At infinite time both hypotheses lead to the same solution, for which the mixed layer potential temperature equals that of the surface and radiative cooling is balanced by entrainment heating.

3. A SHALLOW MOIST CLOUD-TOPPED LAYER IN STEADY-STATE CONDITIONS

The presence of water in two phases adds complications to the previous analysis. A major difficulty lies in relating the first law of thermodynamics to the buoyancy term in the vertical equation of motion. In a dry atmosphere the relationship is straightforward. The potential temperature is both a conservative variable and an appropriate measure of gravitational stability. When we seek such a conservative thermodynamic variable in an atmosphere subject to phase changes we find that it (say, wet-bulb potential temperature) does not necessarily suffice as a measure of buoyancy. That is, if two parcels of air with different wet-bulb potential temperatures are placed side by side, we do not know which is denser unless both are saturated. In the present context this means that: (a) the assumption made in Section 1 on stability of a cloud layer under an inversion, although plausible, is not guaranteed, since it rests on a further assumption that forced mixing between the adjacent layers will occur and bring about a saturated mixed region where the conservative thermodynamic variable then becomes a measure of buoyancy; and (b) the transformation between potential and kinetic energy is porportional, not to the flux of the wet-bulb potential temperature, but to that of an appropriate potential density, or, as we define later, to the flux of virtual potential temperature.

In order to simplify the thermodynamics as much as possible for a mixed layer which is thin compared to the atmospheric scale height, we construct a linearized condensation model. The Clausius-Clapeyron equation, combined with the hydrostatic equation, can be written as a differential relationship between saturation mixing ratio, potential temperature and height, i.e.

$$dq_{sat} = a\, d\theta - b\, dz \quad . \quad . \quad . \quad . \quad . \quad (19)$$

The coefficients a and b are rather rapidly changing functions of temperature and pressure, but we shall consider them as constants over a shallow height interval. We also define the wet-bulb potential temperature, θ_w, as fundamentally a measure of the total sensible plus latent heat content of the air, specifically

$$(1 + \alpha)\, d\theta_w = d\theta + \frac{L}{c_p}\, dq \quad . \quad . \quad . \quad . \quad (20)$$

where $\alpha = aL/c_p$, L and c_p being respectively the latent heat of condensation and specific heat of air at constant pressure (height). By combining the above two expressions we can show that the moist adiabatic lapse rate of θ and q are given by

$$\left(\frac{\partial\theta}{\partial z}\right)_{\theta_w} = \frac{b}{a}\frac{\alpha}{1+\alpha}, \left(\frac{\partial q}{\partial z}\right)_{\theta_w} = -\frac{b}{1+\alpha}$$

and therefore that Eq. (20) can be written also as

$$d\theta_w = d\theta - \left(\frac{\partial\theta}{\partial z}\right)_{\theta_w} dz_c \quad . \quad . \quad . \quad . \quad (21)$$

where z_c is the level of lifting condensation. Direct integration of Eq. (21) shows that the wet-bulb potential temperature can also be defined in the usual way as the temperature produced by lifting a parcel to its condensation level and then dropping it along a moist adiabat to sea-level. As a measure of relative buoyancy we define a virtual potential temperature, θ_v, to include the contributions of both vapour and liquid water to air density,

$$d\theta_v = d\theta + \bar{\theta}\,(\delta\, dq - dl) \quad . \quad . \quad . \quad . \quad (22)$$

where $\delta = 0{\cdot}608$, $\bar{\theta}$ is a reference temperature, and l is the liquid water content.

The above expressions are valid both for mean and fluctuating quantities. The former may be obtained by integration, with constants chosen such that $\theta_w = \theta$ at sea-level saturation and $\theta_v = \theta$ in a dry atmosphere. The latter enter into expressions for the turbulent fluxes, which then may be obtained directly from the above, e.g.

$$(1 + \alpha)\,\overline{w'\theta_w'} = \overline{w'\theta'} + L\,\overline{w'q'}/c_p \quad . \quad . \quad . \quad (23)$$

$$\overline{w'\theta_v'} = \overline{w'\theta'} + \bar{\theta}\,(\delta\,\overline{w'q'} - \overline{w'l'}) \quad . \quad . \quad . \quad (24)$$

As an alternative to the wet-bulb potential temperature we could have used the equivalent potential temperature, θ_e, which, within the present approximation, is defined by

$$d\theta_e = (1 + \alpha)\,d\theta_w \quad . \quad . \quad . \quad . \quad . \quad (25)$$

By use of the above relations and modelling assumptions analogous to those of the previous section time-dependent equations for the moist cloud model have been derived. These derivations appear in a report available on request (Lilly 1967) and the resulting equations are summarized in the right-hand column of Table 1. The basic modelling assumption is that both θ_w and $q + l$ are constant throughout the mixed layer, and that θ and q are also constant beneath the level of the cloud base, at $z = h$. Surface fluxes are related to air-sea differences by the same form of bulk transfer relationship as Eq. (1), and the derivation of Eq. (5) is repeated for the moist cloud variables at the cloud top. The first four rows in the right of Table 1 contain the resulting expressions.

The entrainment conditions necessary to close the system for either time-dependent or steady-state solutions are chosen in exact analogy with the dry case except for the use of virtual temperature flux, since that is the appropriate energy transformation function for this case. These are

$$\text{Maximum}: \int_0^H \overline{w'\theta_v'}\,dz = 0, \qquad \text{but} \quad \overline{w'\theta_v'} \neq 0 \quad \text{somewhere}. \quad (26)$$

$$\text{Minimum}: \quad (\overline{w'\theta_v'})_{\text{minimum}} = 0, \quad \text{but} \int \overline{w'\theta_v'}\,dz > 0. \quad . \quad . \quad (27)$$

In order to evaluate these we must express $\overline{w'\theta_v'}$ in terms of the conservative variables. Elimination of the potential temperature flux between Eqs. (23) and (24) leads to the expression

$$\overline{w'\theta_v'} = (1 + \alpha)\,\overline{w'\theta_w'} - \bar{\theta}\,\overline{w'(q' + l')} - \left[\frac{L}{c_p} - \bar{\theta}\,(\delta + 1)\right]\overline{w'q'} \quad . \quad (28)$$

In the sub-cloud layer the liquid water-flux vanishes. In the cloud we may use Eqs. (19) and (21), evaluated at a constant height, to show that $\overline{w'q'} = a\,\overline{w'\theta_w'}$, and this allows the first and last terms on the right-hand side of Eq. (28) to be combined. Thus we obtain

$$\overline{w'\theta_v'} = \begin{cases} (1 + \alpha)\,\overline{w'\theta_w'} - \left(\dfrac{L}{c_p} - \bar{\theta}\delta\right)\overline{w'q'}, & z < h \\ [1 + a\bar{\theta}\,(\delta + 1)]\,\overline{w'\theta_w'} - \bar{\theta}\,\overline{w'(q' + l')}, & z > h \end{cases} \quad . \quad . \quad (29)$$

which can immediately be evaluated in terms of boundary quantities since each of the component flux terms has the same linear form as Eq. (3).

The maximum entrainment condition, obtained by carrying out the integration of Eg. (26), is shown in the right-hand column of Table 1, where

$$\alpha_1 = \frac{\alpha - a\bar{\theta}\,(\delta + 1)}{1 + a\bar{\theta}\,(\delta + 1)}, \quad \beta_1 = \frac{a\bar{\theta}}{1 + a\bar{\theta}\,(\delta + 1)}. \quad . \quad . \quad . \quad (30)$$

The effects of the use of virtual temperature in this and subsequent expressions can be traced by noting that if $\overline{w'\theta'}$ were used instead of $\overline{w'\theta_v'}$, α_1 would reduce to α and β_1 to

TABLE 1. SUMMARIZED PROPERTIES OF DRY AND WET MODELS

Dry cloud	Assumptions and basic equations	Wet cloud
$\theta = \theta_0$	Mixed layer assumption, $z < H$	$\theta_w = \theta_{w0}, \quad q + l = q_0$
$\frac{\partial \theta_0}{\partial t} = [\overline{(w'\theta')}_0 - \overline{(w'\theta')}_H]/H$	Mixed layer budget equations	$\frac{\partial \theta_{w0}}{\partial t} = [\overline{(w'\theta_w')}_0 - \overline{(w'\theta_w')}_H]/H$ $\frac{\partial q_0}{\partial t} = [\overline{(w'q')}_0 - \overline{w'(q'+l')}_H]/H$
$\overline{(w'\theta')}_0 = C_T V_0 (\theta_s - \theta_0)$	Surface flux assumptions	$\overline{(w'\theta_w')}_0 = C_T V_0 (\theta_{wS} - \theta_{w0})$ $\overline{(w'q')}_0 = C_T V_0 (q_S - q_0)$
$\left(\frac{\partial H}{\partial t} - w_H\right)(\theta_{UH} - \theta_0) + \overline{(w'\theta')}_H = F_{UH}$	Cloud top conditions	$\left(\frac{\partial H}{\partial t} - w_H\right)(\theta_{wUH} - \theta_{w0}) + \overline{(w'\theta_w')}_H = \frac{F_{UH}}{1+\alpha}$ $\left(\frac{\partial H}{\partial t} - w_H\right)(q_{UH} - q_0) + \overline{w'(q'+l')}_H = 0$
$\overline{(w'\theta')}_H = -\overline{(w'\theta')}_0$	Maximum entrainment condition	$\left(1+\alpha_1\frac{h^2}{H^2}\right)\overline{(w'\theta_w')}_H - \left(\beta_1+\alpha_1\frac{h^2}{H^2}\right)\frac{\overline{w'(q'+l)}_H}{a} =$ $-\left[1+\alpha_1\frac{h}{H}\left(2-\frac{h}{H}\right)\right]\overline{(w'\theta_w')}_0 + \left[\beta_1+\alpha_1\frac{h}{H}\left(2-\frac{h}{H}\right)\right]\frac{\overline{(w'q')}_0}{a}$
$\overline{(w'\theta')}_H = 0$	Minimum entrainment condition	Smallest of $\left\{\begin{array}{l}(1+\alpha)\overline{w'\theta_w'} - \left(\frac{L}{c_p} - \bar{\theta}\delta\right)\overline{w'(q'+l')}, \; z < h \\ [1+\alpha\bar{\theta}(\delta+1)]\overline{w'\theta_w'} - \bar{\theta}\,\overline{w'(q'+l')}, \; z > h\end{array}\right\} = 0$
None ($h = 0$)	Cloud base condition	$h = \frac{q_{s0} - q_0}{b}$

zero. The cloud base level h is evaluated by integrating Eq. (19) upwards from the sea surface, and the result may be expressed in various alternative forms by the use of Eqs. (20) and (21), e.g.

$$bh = q_S - q_0 - a(\theta_S - \theta_0) = (1 + \alpha)[q_S - q_0 - a(\theta_{wS} - \theta_{w0})] = q_{s0} - q_0 \quad (31)$$

where q_{s0} is the saturation humidity of surface air at temperature θ_0. In order to determine the minimum entrainment condition it is necessary to locate the minimum value of Eq. (29) and then set it to zero. In general this could occur at one of four places, the bottom or top of the sub-cloud or cloud layer.

We now restrict our attention to the steady-state, for the purpose of comparison of theory with observational data from a region of, hopefully, only slowly changing conditions. In the steady-state the upper and lower boundary fluxes of wet-bulb potential temperature and total moisture content are equal, and the relations in the second, third and fourth rows of Table 1 can be reduced to

$$\omega(\theta_{wUH} - \theta_{w0}) + \theta_{wS} - \theta_{w0} = \frac{F_{UH}}{C_T V_0 (1 + \alpha)} \quad . \quad . \quad . \quad (32)$$

$$\omega(q_{UH} - q_0) + q_S - q_0 = 0 \quad . \quad . \quad . \quad . \quad . \quad . \quad (33)$$

where $\omega = -w_H/C_T V_0$. For purposes of comparison with observational data it is also convenient to use a similar expression in terms of potential temperature, obtained from subtracting Eq. (33) from Eq. (32) with the aid of Eq. (20):

$$\omega(\theta_{UH} - \theta_0) + \theta_S - \theta_0 = F_{UH}/C_T V_0 \quad . \quad . \quad . \quad . \quad (34)$$

The maximum entrainment condition reduces to a greatly simplified form

$$(1 + \alpha_1 h/H)\, a(\theta_{wS} - \theta_{w0}) = (\beta_1 + \alpha_1 h/H)(q_S - q_0) \quad . \quad . \quad (35)$$

or the equivalent, using θ-differences.

$$(1 + \alpha_1 h/H)\, a(\theta_S - \theta_0) = [\beta_1 - \alpha(1 - \beta_1) + \alpha_1 h/H](q_S - q_0). \quad . \quad (36)$$

In order to determine the location of the minimum θ_v flux we take the difference of the two expressions in Eq. (29), i.e.

$$\begin{aligned} \overline{(w'\theta_v')}_{z<h} - \overline{(w'\theta_v')}_{z<h} &= \frac{\alpha_1}{\beta_1}[a\,\overline{w'\theta_w'} - \overline{w'(q' + l')}] \\ &= \frac{\alpha_1}{\beta_1} C_T V_0 [a(\theta_{wS} - \theta_{w0}) - (q_S - q_0)] \quad . \quad (37) \\ &= -\frac{\alpha_1 C_T V_0}{\beta_1 (1 + \alpha_1)} bh \end{aligned}$$

where the bulk transfer expressions have been used for evaluating the fluxes and Eq. (31) substituted into the final equality. This shows that the virtual potential temperature flux is smallest in the sub-cloud layer. The minimum entrainment condition thus becomes simply vanishing of the air-sea virtual temperature difference, i.e.

$$\theta_{vS} = \theta_{v0} \quad . \quad . \quad . \quad . \quad . \quad . \quad (38)$$

or the equivalent, from Eq. (22),

$$\theta_S - \theta_0 = -\bar{\theta}\delta(q_S - q_0). \quad . \quad . \quad . \quad (39)$$

These results show some interesting features exclusive to the moist cloud model. In the steady-state, and presumably for small deviations from it, the cloud layer is maintained in active convection, with upward virtual heat-flux. The sub-cloud layer, on the other hand, is driven, with a downward virtual heat-flux and the surface air virtually warmer than the sea (assuming that the observed state lies between the maximum and minimum entrainment models). The source of the convective energy released in the cloud layer is the latent heat of water evaporated from the sea surface and re-condensed at the cloud base, while sensible heat is actually transported downwards into the sea. This effect is consistent with the observations of air temperature higher than sea surface temperature in the summertime eastern Pacific near the California coast (Weather Bureau and Hydrographic Office 1961).

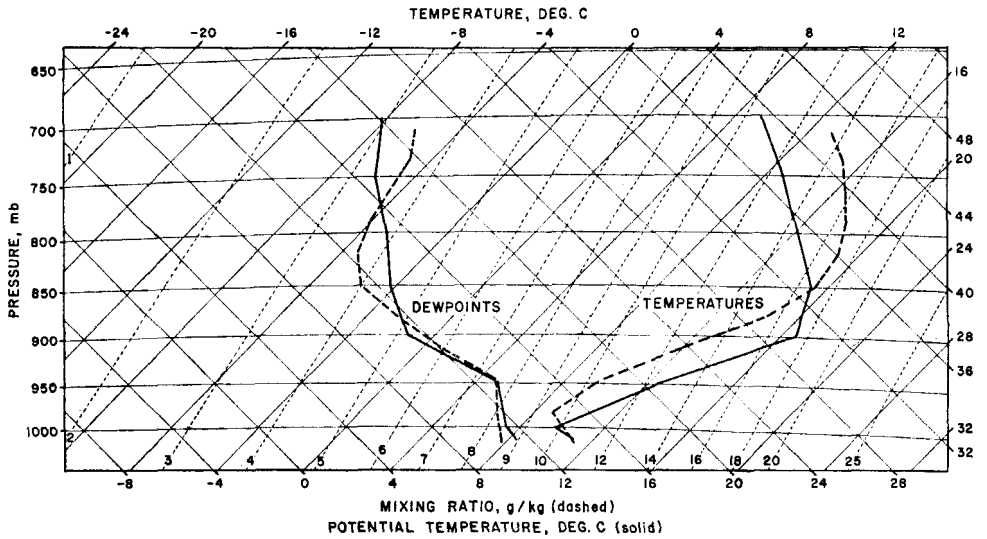

Figure 2. Mean atmospheric sounding for Oakland, California, August, 1963-66 (solid lines); mean of 27 daily airplane meteorograph records from Walvis Bay, South West Africa, taken during October 1939 (dashed lines).

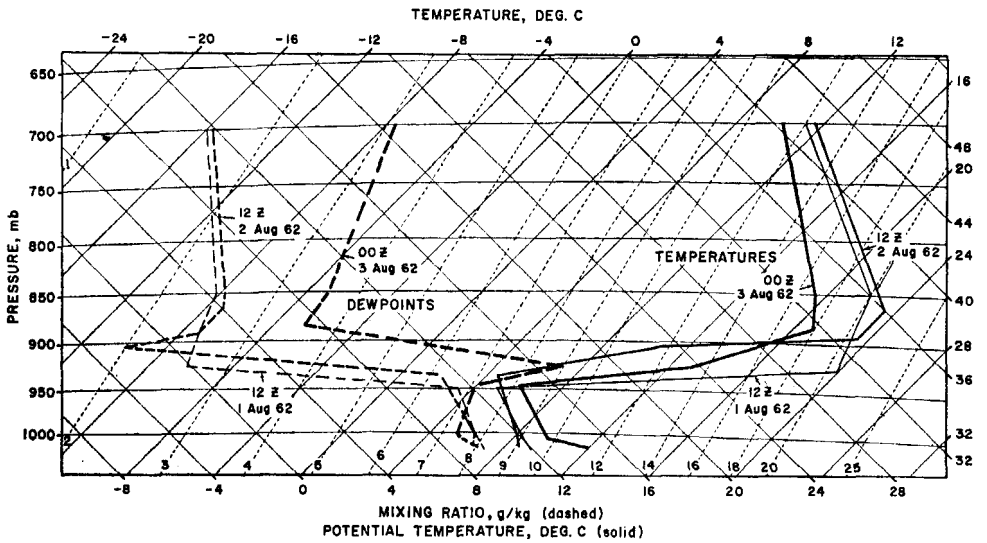

Figure 3. Radiosonde observations from Oakland, California, 1-3 August 1962.

4. Comparison with observations

Figs. 2 and 3 show some examples of the ordinarily available data. In Fig. 2 the mean sounding for Oakland, California, for August, 1963-66, is plotted, together with that for a month of airplane ascents at Walvis Bay, South West Africa, in October, 1939 (Taljaard and Schumann 1940). The old airplane data might be somewhat more accurate in strong inversion situations than those of modern radiosondes because the slower climb rate of the airplane allowed more time for instrumental response. The individual meteorograph records are, however, no longer available. July and August are the months of maximum frequency of low ceilings at Oakland, while the régime is present persistently throughout the year at Walvis Bay. Comparison of the mean soundings suggests that circumstances in the two areas are similar. Fig. 3 exhibits soundings from Oakland for three consecutive days in August 1962. On each of these days stratus overcasts were reported with ceilings at 200-300 or 300-600 meters, and also light drizzle was reported in two cases, with less than 0·01 inch accumulation. It is important to note that the humidity data are somewhat inadequate in both the mixed layer and the upper dry layer. No saturation humidities were reported in the cloud and in some of the upper levels the instrument was 'motorboating' and unable to measure humidity correctly.

In Fig. 4 we have plotted the wet-bulb potential temperature and mixing ratio for each of the 1-3 August 1962 soundings. In the inversion region these have been adjusted in an attempt to compensate for some of the instrumental errors obviously present. The adjustments mostly consisted of raising the temperature and lowering the humidity in the apparent inversion zone in such a way that the wet-bulb potential temperature and mixing ratio varied smoothly above and below a narrow transition layer. Admittedly this is partially forcing the theory onto the data, but it seems partly supported by the results of recent airplane soundings (Edinger 1963, 1966) and slow-ascent radiosondes (Williams and de Mandel 1966), neither of which, however, included humidity data. The region of adjustment is indicated by dashed lines. No attempt was made to alter the mixed layer humidity to require saturation within the cloud, since this would seem to require increasing the mixing ratio in some cases to greater than surface values. In

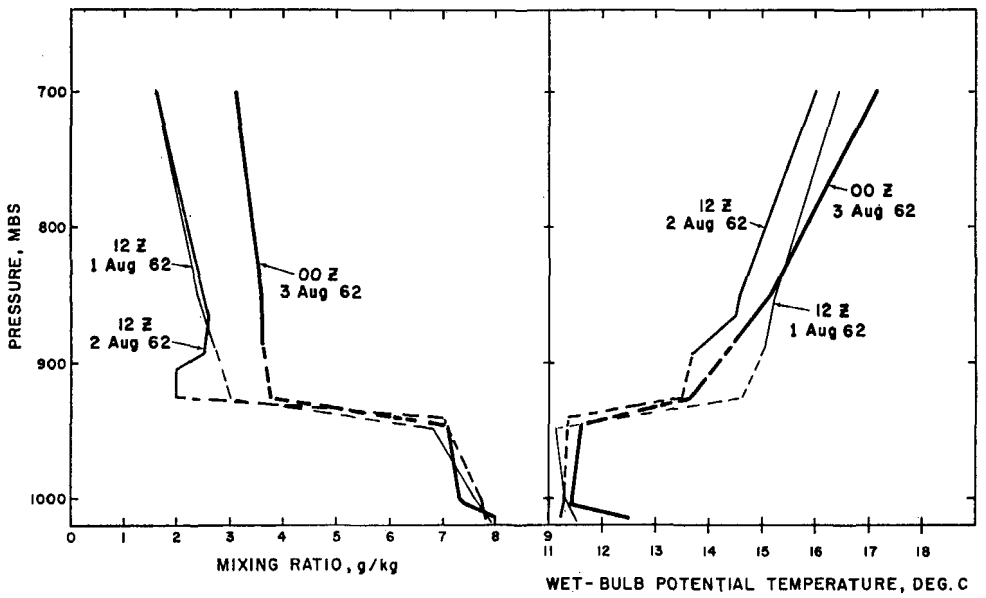

Figure 4. Wet-bulb potential temperature and mixing ratio obtained from the data of Fig. 3. The dashed areas indicate regions where the data have been adjusted somewhat to remove apparent lags in the humidity record and wet-bulb effects in the temperature record in the inversion region.

the dry layer above the inversion region, when 'motorboating' occurred, humidity was assumed to correspond to the station averages used by the U.S. Weather Bureau for that situation. From the average of the adjusted soundings the following parameters were abstracted.

$$q_0 = 7{\cdot}8 \text{ g/kg}, \quad q_{UH} = 3{\cdot}0 \text{ g/kg}, \quad \theta_0 = 13{\cdot}3°\text{C}, \quad \theta_{UH} = 31{\cdot}8°\text{C},$$

$$\theta_{w0} = 11{\cdot}4°\text{C}, \quad \theta_{wUH} = 13{\cdot}6°\text{C}, \quad q_{s0} = 9{\cdot}6 \text{ g/kg}, \quad H = 620 \text{ m} \quad . \qquad (40)$$

The sea-surface temperature, θ_S, and its associated saturation mixing ratio, q_S, the ventilation factor, $C_T V_0$, and the subsidence rate, $-w_H$, are probably the least well known parameters for the present data. This is principally because the station, Oakland, is located directly downwind of San Francisco Bay, a rather large body of water whose temperature is several degrees higher than that of the open sea some 15 miles upwind. The most appropriate surface temperature is therefore somewhat uncertain. Besides the general uncertainty of the bulk transfer coefficient C_T the wind speed itself is highly variable spatially along the California coast and has a strong diurnal oscillation. The same spatial and temporal variability leads to difficulties in estimating low-level divergence and subsidence rates from the usual synoptic or even climatological data.

We therefore use the data of Eq. (40) to predict values of the more uncertain parameters. From integration of Eq. (19) at constant z, we can obtain a formula relating q_S to θ_S

$$q_S = q_{s0} + a(\theta_S - \theta_0). \quad . \quad . \quad . \quad . \qquad (41)$$

Upon substitution of Eq. (41) into the maximum and minimum entrainment conditions of Eqs. (36) and (39), we get expressions for the sea surface temperature,

$$\text{Maximum}: \theta_S = \theta_0 - \frac{q_{s0} - q_0}{a}\left[1 - \frac{1 + \alpha_1 (q_{s0} - q_0)/bH}{(1 + \alpha)(1 - \beta_1)}\right] \quad . \qquad (42)$$

$$\text{Minimum}: \theta_S = \theta_0 - \frac{q_{s0} - q_0}{a}\frac{a\bar{\theta}\delta}{1 + a\bar{\theta}\delta} \cdot \quad . \quad . \quad . \qquad (43)$$

The above results may then be substituted into Eqs. (33), (34) and (31) in order to evaluate ω, $F_{UH}/C_T V_0$, and h. Table 2 contains the results of these evaluations. The coefficients a, b, α, α_1, and β_1 were computed for a reference temperature equal to θ_0, 13·3°C, which was also used in place of $\bar{\theta}$.

The two sets of computed results are surprisingly close. The predicted air-sea differences are well within the observational uncertainty – perhaps they would be so even in a carefully conducted observation study in open sea conditions. If the cloud top radiation flux and surface wind velocities were known adequately, the fourth entry in Table 2 might show separation adequate to allow a choice. Therefore calculations were made by several methods for the net radiative flux off the cloud top.

TABLE 2. MODEL PREDICTIONS FOR THE DATA OF EQ. (40), MADE FROM RADIOSONDE DATA OF OAKLAND, CALIFORNIA, 1-3 AUGUST 1962

Quantity	Equations	Maximum entrainment	Minimum entrainment
$\theta_0 - \theta_S$	(42), (43)	0·75°C	0·28°C
$q_S - q_0$	(41)	1·31 g/kg	1·62 g/kg
$\omega = -w_H/C_T V_0$	(33)	0·21	0·28
$F_{UH}/C_T V_0$	(34)	2·9°C	4·8°C
h	(31)	345 m	345 m

Coefficients: $a = 0{\cdot}652 \times 10^{-3}$ deg^{-1}, $b = 0{\cdot}522 \times 10^{-5}$ m^{-1}, $\alpha = 1{\cdot}60$, $\alpha_1 = 1{\cdot}00$, $\beta_1 = 0{\cdot}144$

If the cloud can be considered black to terrestrial radiation then the radiation calculation consists of (a) upward radiation flux from a black-body at the temperature of the cloud top; (b) downward flux from the inversion region and beyond; (c) solar radiation flux absorbed by the cloud and mixed layer. Regarding the question of blackness, calculations were made by use of the experimental data of Saito (1956) and the theoretical study of Yamamoto, Tanaka and Kamitani (1966). Upon assuming a moist adiabatic distribution of liquid water, from Saito's data we computed 99 per cent absorption of unreflected incident radiation at a cloud layer depth of 124 meters, and the same from the Yamamoto, *et al.* model at 156 meters. The latter model also predicts a long-wave reflectivity of 3·5 per cent and computed net black-body fluxes were therefore reduced by that amount.

TABLE 3. SOUNDING ASSUMED FOR RADIATION COMPUTATIONS, CLOUD TOP AT 945 mb

p mb	T deg K	q g/kg
945	282·8	8·0
940	291·4	5·5
935	299·9	3·0
925	298·9	3·0
900	297·6	2·89
850	294·4	2·67
800	291·1	2·44
750	287·7	2·22
700	284·1	2·00
600	275·1	1·60
500	265·5	1·10
400	253·1	0·50
300	237·4	0·15
200	216·1	0·02
150	208·1	0·01

The black-body upward and downward long-wave fluxes were computed principally from the assumed sounding of Table 3, one similar to the average of the August cases, but with an inversion thickness of 10 mb. However, some calculations were also made with inversion thickness from 5 to 20 mb, with little change in the results. Computations of the downward flux were made by use of the emissivity graphs published by Manabe and Wetherald (1967), the tables of Elsasser and Culbertson (1960), and those of Yamamoto (1952). For the latter two the computations were made using a computer model kindly made available by Dr. T. Sasamori, while the Manabe-Wetherald computations were done more crudely by hand. In addition the flux associated with water vapour lines was also calculated from observationally determined emissivity data published by Kuhn (1963) and Brooks (1950). All of these results are summarized on Table 4. From these it is clear that the Manabe-Wetherald and Sasamori-Yamamoto results are almost identical, which is understandable since the emissivities used in the former are very similar to those of Yamamoto. The large differences between these two and the Elsasser-Culbertson computations are caused by substantial differences in absorptivities over moderate water vapour path lengths, 0·1-1·0 g cm^2, accentuated by the strong inversion in the assumed sounding.

Solar radiation absorption was computed by use of the Manabe-Strickler (1964) clear air depletion values and Neiburger's (1949) observational value of 7 per cent cloud absorption, which also appears to be consistent with recent calculations by Twomey, Jacobwitz and Howell (1967). The high noon value computed was 0·109 ly/min, the daytime average 0·052 ly/min, and the 24-hour average 0·032 ly/min, all for July.

TABLE 4. COMPUTATION OF LONG-WAVE RADIATION FLUX

	Manabe-Wetherald	Sasamori-Yamamoto	Elsasser-Culbertson	Kuhn	Brooks
Total downward water vapour flux	0·363 ly/min	0·362	0·283 ly/min	0·310 ly/min	0·321
Additions from CO_2 overlap	0·048	0·046	0·060		
Total downward flux	0·411	0·408	0·343		
Upward black-body flux	*0·521*	*0·521*	*0·521*		
Net upward flux	0·110	0·113	0·178		

T. Sasamori has recently made comparisons of Elsasser-Culbertson and Yamamoto model results with observed fluxes made in Japan, and the results of these comparisons (Sasamori 1968) have convinced the author that the latter model is considerably better. For the present estimate, however, we have taken an algebraic average of the first three columns of Table 4 and obtained a net upward flux, assuming a black-body cloud, of 0·134 ly/min. After reducing this by 3·5 per cent for the reflectivity, and by 0·032 ly/min for the 24-hour averaged solar absorption, we obtained the final value for the computed radiative heat loss from the cloud top, $\rho c_p F_{UH} = 0{\cdot}097$ ly/min, or $F_{UH} = 0{\cdot}055$ deg m sec^{-1}. Upon assuming $C_T = 0{\cdot}0015$, V_0 is predicted to be 12·6 or 7·6 m sec^{-1}, respectively, for the maximum or minimum entrainment model. The first of these is apparently too large; the second also seems, if anything, rather on the high side. A tentative conclusion is, therefore, that the minimum entrainment model conforms best with observations. The various uncertainties in the radiation flux, heat transport coefficient, steadiness and representativeness of the station conspire against more definite conclusions. The subsidence rate, for the above parameters, is 0·40 cm sec^{-1} for the

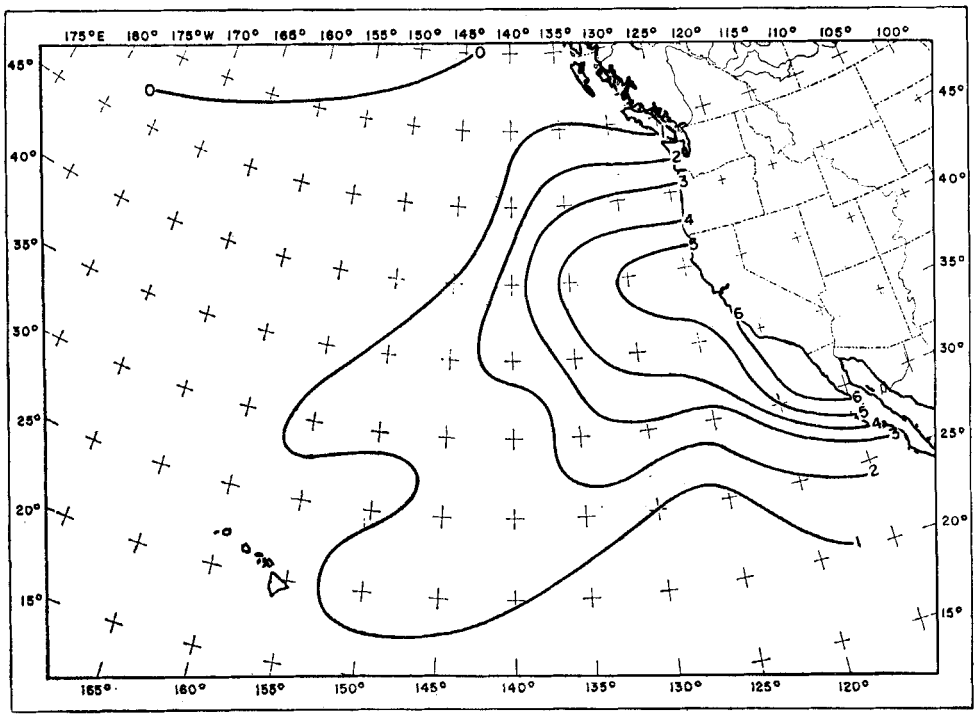

Figure 5. Divergence of surface resultant winds in July, units of 10^{-6} sec^{-1} (from Neiburger *et al.* 1961).

maximum entrainment model and 0·32 cm sec^{-1} for the minimum, corresponding to a mixed layer average divergence rate of $6{\cdot}5 \times 10^{-6}$ sec^{-1} or $5{\cdot}2 \times 10^{-6}$ sec^{-1} respectively. Again, the smaller figures are preferable, about equalling the July average surface divergence near San Francisco Bay as shown by Neiburger, Johnson and Chien (1961), whose map has been reproduced as Fig. 5.

5. Conclusion and outlook

The steady-state model described above appears to be reasonably successful in relating, explaining and predicting many of the features of observed cloud layers. The prediction of a positive vertical gradient of θ_w in the inversion seems to agree with observational data. The computed radiative cooling rates, although insufficiently certain for the most effective use, are of such a magnitude that the predicted horizontal and vertical wind velocities seem reasonable. The sea surface temperature is predicted to be slightly cooler than that of the air near the surface, in general agreement with climatological atlas data for the eastern Pacific. Perhaps the most important result is that the choice of an entrainment hypothesis, at least within the postulated limits, is not critical to the existence or general character of the steady-state solutions.

One may perhaps go further and conjecture that the strong inversions typical of the so-called 'marine layer' of coastal California and similar regions are necessarily maintained by a low cloud layer in the manner described above. It would appear impossible for any observed combination of subsidence, convection, and shearing turbulence to produce sufficient amounts of kinetic energy to maintain a 15-20 degree inversion at a height of 500-1,000 meters without a radiatively effective cloud cover. Clear skies or patchy clouds are often observed in the presence of such strong inversions, but this is probably a transient state produced by rapid changes of radiation, surface temperatures or subsidence, especially those associated with diurnal sea-breeze circulations. Further investigation of such transients could be accomplished by numerical solution of the time-dependent model equations.

If the above conjecture is correct then the proposed model is a partial solution to the often discussed question of the origin of the trade wind inversion. In a sense the model only pushes the problem back one step and substitutes the question of origin of the cloud layer which must be present at the time subsidence commences. This original cloud layer might be a remnant of the frontal disturbances that frequently pass through the Gulf of Alaska in summer, or it may simply be produced from evaporative moistening of a previously clear mixed layer.

Additional subjects for future investigation are the conditions and mechanisms of break-up of the cloud layer at its equatorward end into the characteristic tropical cumulus population. Meteorological satellite observations indicate that this break-up frequently includes a stage during which meso-scale cell structures are observed (Krueger and Fritz 1961). Similar cells may also occur without solid cloud layers upwind. The principles of the present analysis may perhaps also be applied to an investigation of the cell mechanics.

It seems useful to speculate on the form of an observational study designed to test more thoroughly the above theoretical results. Assuming at least once-daily satellite coverage to establish the large-scale cloud structure and sufficient surface data from 'ships of opportunity' and land stations adequately to define the surface pressure field and at least allow estimates of low-level divergence, an ideal observational study could probably be conducted with the use of one stationary ship for a week to ten days plus an instrumented airplane for not over a month. The ship should be capable of flying a tethered balloon with a telemetered thermometer, hygrometer, and net radiometer suspended from it and slowly raised and lowered through the cloud layer and inversion regions. Adequate wind velocity and air and sea-surface temperature and/or heat and moisture flux measurements should be made from the ship. The airplane should be equipped for measuring liquid

water and turbulent intensity or dissipation. The airplane observations would serve to check the spatial representativeness of the shipboard data, and the ship soundings could establish the time variability when both plane and ship were available. It would be important to have both day and night soundings to obtain data on the important diurnal changes caused by radiation and sea-breeze cycles.

Acknowledgments

A significant portion of the work reported here was done during a visit to the National Hurricane Research Laboratory at Miami in 1965, for which opportunity I am grateful to those who made it possible. I am indebted also to P. M. Saunders and T. Sasamori for the benefit of several frank and helpful discussions and especially for their assistance in the radiative aspects. Finally, I would like to credit J. S. Turner and his collaborators at the Woods Hole Oceanographic Institution and elsewhere, with providing, in recent papers not referred to above (especially Turner and Yang 1963, Turner and Kraus 1967) and in private communications over the past several years, much of the experimental and theoretical background for the methods used in this study.

References

Ball, F. K.	1960	'Control of inversion height by surface heating,' *Quart. J. R. Met. Soc.*, **86**, p. 483.
Brooks, D. L.	1950	'A tabular method for the computation of temperature change by infra-red radiation in the free atmosphere,' *J. Met.*, **7**, p. 313.
Deardorff, J. W., Willis, G. E. and Lilly, D. K.	1968	'Laboratory investigation of non-steady penetrative convection,' submitted to *J. Fluid Mech.* Available from the authors as N.C.A.R. manuscript No. 68-72.
Edinger, J. G.	1963	'Modification of the marine layer over coastal California,' *J. Appl. Met.*, **2**, pp. 706-712.
	1966	'Wave clouds in the marine layer upwind of Pt. Sal., California,' *Ibid.*, **5**, pp. 804-809.
Elsasser, W. M. and Culbertson, M. R.	1960	*Atmospheric radiation tables, Met. Mon.* **4**, No. 23, American Meteorological Society, Boston, 43 pp.
Ficker, H. von	1936	'Die Passatinversion,' *Veroff. Meteor. Inst., Berlin*, **1**, p. 5.
James, D. G.	1959	'Observations from aircraft of temperatures and humidities near stratocumulus clouds,' *Quart. J. R. Met. Soc.*, **85**, p. 120.
Krueger, A. F. and Fritz, S.	1961	'Cellular cloud patterns revealed by Tyros I,' *Tellus*, **13**, pp. 1-7
Kuhn, P. M.	1963	'Radiometersonde observations of infrared flux emissivity of water vapour,' *J. Appl. Met.*, **2**, pp. 368-378.
Lilly, D. K.	1967	'Models of cloud layers under a strong inversion,' NCAR Manuscript No. 386, National Center for Atmospheric Research, Boulder, Colorado.
Manabe, S. and Strickler, R.	1964	'Thermal equilibrium of the atmosphere with a convective adjustment,' *J. Atmos. Sci.*, **21**, p. 361.
Manabe, S. and Wetherald, R. T.	1967	'Thermal equilibrium of the atmosphere with a given distribution of relative humidity,' *Ibid.*, **24**, p. 241.
Neiburger, M.	1944	'Temperature changes during formation and dissipation of west coast stratus,' *J. Met.*, **1**, p. 29.
	1949	'Reflection, absorption and transmission of isolation by stratus cloud,' *Ibid*, **6**, p. 98.
Neiburger, M., Johnson, D. S. and Chien, C.	1961	*Studies over the Eastern Pacific Ocean in summer, I, The inversion over the Eastern North Pacific Ocean.* University of California Publications in Meteorology, **1**, No. 1.
Ogura, Y. and Phillips, N. A.	1962	'Scale analysis of deep and shallow convection in the atmosphere,' *J. Atmos. Sci.*, **19**, p. 173.
Petterssen, S.	1938	'On the causes and forecasting of the California fog,' *Bull. Amer. Met. Soc.*, **19**, p. 49.

Richards, J. M.	1963	' Experiments on the motion of isolated cylindrical thermals through unstratified surroundings,' *Internat. J. Air Water Pollution*, **17**, p. 17.
Riehl, H.	1954	*Tropical meteorology*, McGraw Hill, New York.
Saito, T.	1956	*Measurement of transmissivity of infra-red radiation through fog*, Sci. Rep. of Tohoku University, Series 5, **8**, p. 53.
Sasamori, T.	1968	' The radiative cooling calculation for application to general circulation experiments,' to be published in *J. Appl. Met.*, **8**, October issue. Also available from the author as N.C.A.R. manuscript No. 68-37.
Taljaard, J. J. and Schumann, T. E. W.	1940	' Upper-air temperatures and humidities at Walvis Bay, Southwest Africa,' *Bull. Amer. Met. Soc.*, **21**, p. 293.
Twomey, S., Jacobwitz, H. and Howell, H. B.	1967	' Light scattering by cloud layers,' *J. Atmos. Sci.*, **24**, p. 70.
Weather Bureau and Hydrographic Office	1961	*Climatological and Oceanographic Atlas for Mariners, Vol. II*, U.S. Government Printing Office, Washington, D.C.
Williams, W. A. and De Mandel, R. E.	1966	*Land-sea boundary effects on small-scale circulations*, San Jose State College Progress Report No. 2, National Science Foundation Grant GP-4248.
Yamamoto, G.	1952	*On a radiation chart*, Sci. Rep. of Tohoku University Series 5, **4**, p. 9.
Yamamoto, G., Tanaka, M. and Kamitani, K.	1966	' Radiative transfer in water clouds in the 10-micron window region,' *J. Atmos. Sci.*, **23**, p. 305.